Inorganic Chemistry

ARTICLE

pubs.acs.org/IC

A Vanadium (VO^{2+}) Metal−Organic Framework: Selective Vapor Adsorption, Magnetic Properties, and Use as a Precursor for a Polyoxovanadate

Prakash Kanoo,[‡] Ashta Chandra Ghosh,[‡] and Tapas Kumar Maji*

Molecular Materials Laboratory, Chemistry and Physics of Materials Unit, Jawaharlal Nehru Centre for Advanced Scientific Research, Jakkur, Bangalore 560 064, India

Supporting Information

ABSTRACT: The reaction of $VOSO_4$ with 2-carboxyethylphosphonic acid (H_2-CEP) in presence of piperazine (PIP) produces a 3D inorganic−organic hybrid framework, $\{(H_2PIP)_{0.5}[VO(CEP)]\cdot H_2O\}$ (**1**) with bidirectional channels occupied by the H_2PIP cations and H_2O molecules. The PO_3^{2-} unit of CEP connects three V^{IV} centers to generate a 1D ladder, which is further linked to four such ladders by the CEP linkers to form a 3D hybrid framework. The dehydrated framework, $\{(H_2PIP)_{0.5}[VO(CEP)]\}$ (**1′**) shows selective and gated adsorption behavior with H_2O but not with methanol and ethanol. Very interestingly, when **1** is treated with an aqueous solution of $LiNO_3/NaNO_3$, the framework breaks down and results in a new polyoxovanadate (POV) cluster, $[H_5(H_2PIP)_3][V^{V}_{12}V^{IV}_{2}O_{38}(PO_4)]\cdot 8H_2O$ (**2**) at pH ≈ 2.1. The cluster has been characterized by single-crystal X-ray diffraction, ^{31}P NMR, EPR, and magnetic studies. The temperature-dependent magnetic susceptibility measurement suggests antiferromagnetic ordering in **1** with $T_N \approx 3.8$ K.

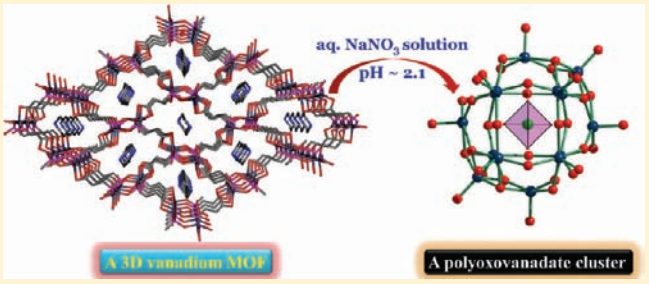

INTRODUCTION

Metal−organic frameworks (MOFs) or porous coordination polymers (PCPs) are crystalline hybrid materials and are strategically constructed by linking metals, metalloligands, or metal clusters with bridging organic linkers.[1] MOFs with regular and tunable pore structure are very attractive for many practical applications, such as gas storage, selective adsorption, separation, catalysis, exchange processes, sensing, and drug delivery.[2−8] Realizing the enormous means of combining metals and ligands, the syntheses of MOFs have a very wide scope, and this is reflected in the current literature, which display a wide variety of structures. Although the last statement holds good for most of the first row transition metals, to our surprise, reports on vanadium MOFs (VMOFs) are scanty in the literature.[9] During the early period of the last decade, Férey and co-workers have reported structures of few VMOFs (e.g., MIL-26 and MIL-47), which they synthesized under hydrothermal conditions.[9a,10] At a later stage, MIL-47 has been explored for several applications, for example, separation of xylene isomers, incorporation of metallocenes, etc.[11] A couple of reports appeared in the middle of the last decade that describe the use of phosphonates and organodiphosphonates for the construction of vanadium open frameworks.[9b−d] A few reports also exist where synthesis and characterization of mixed metal (vanadium and other metal) frameworks have been reported.[9d,12] Because of the high nuclear charge of vanadium (+3, +4, and +5), VMOFs show structural rigidity and robustness and hence exhibit many interesting electronic and magnetic properties.[10]

Apart from this, recently polyoxovanadate (POV) clusters, a class of polyoxometalates (POMs), have also been used as a linker for fabricating functional vanadium framework structures.[12e,f,13] POM clusters are an interesting class of compounds because of their versatile electronic and magnetic properties and also exhibit potential applications in biology and catalysis.[14] Mixed-valent POV/POM clusters have evoked considerable interest because these molecular fragments encapsulate charged or neutral species that function as structure directors in the self-organization process of the formation of the metal oxide cage; they can also be good model systems in the design of complex materials intermediate between molecular compounds and infinite solids. Although, several reports have appeared in the literature on the construction of MOFs from POMs, to the best of our knowledge, the other way, that is, POMs from MOFs, has never been realized.[12b,15]

In this work, we report a VMOF, $\{(H_2PIP)_{0.5}[VO(CEP)]\cdot H_2O\}$ (**1**), which has been synthesized using a bifunctional ligand, 2-carboxyethylphosphonic acid (H_2-CEP) under hydrothermal conditions and autogenous pressure. The compound shows selective adsorption of water vapor over organic solvents at ambient temperature. Moreover, the presence of an unpaired electron in the d-orbital of V^{4+} gives rise to interesting magnetic properties, and the compound orders antiferromagnetically below

Received: March 7, 2011
Published: May 10, 2011

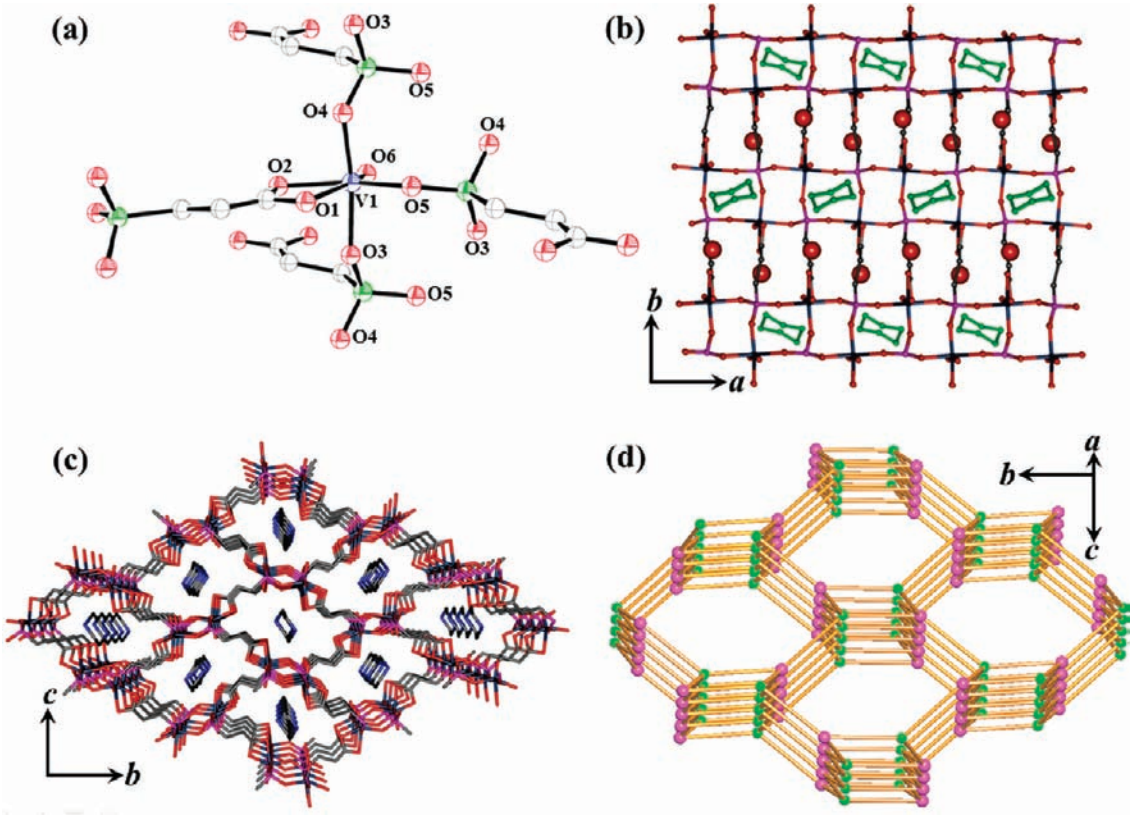

Figure 1. (a) View of the coordination environment of V in framework **1**. Color specifications: vanadium, blue; phosphorus, green; oxygen, red; carbon, gray. (b) View along crystallographic *c* direction (green color molecules imply piperazine cations); guest water molecules are shown as large balls. (c) 3D view of compound **1** showing H_2-PIP molecules in the channels along the *a* direction. Color specifications for panels b and c: vanadium, sky blue; phosphorus, pink; oxygen, red; carbon, gray; nitrogen, blue. (d) Schematic representation of the four-connected net; the green balls represent V1 nodes, and pink balls represent the four-connected ligand CEP.

3.8 K. Further, here we employ a top-down approach to fabricate a POV cluster, $[H_5(H_2PIP)_3][V^V_{12}V^{IV}_2O_{38}(PO_4)]\cdot 8H_2O$ (**2**), by dismantling the VMOF **1** in aqueous medium and at low pH, ~2.1. To establish that use of the framework **1** is the prerequisite for the formation of the POV, experiments have been carried out by mixing the components of MOF **1** with $NaNO_3/LiNO_3$ and to our anticipation the latter did not yield any POV.

RESULTS AND DISCUSSION

Synthesis and Structure of $\{(H_2PIP)_{0.5}[VO(CEP)]\cdot H_2O\}$ (1). In general, synthesis of higher dimensional MOFs in presence of water or other coordinating solvents is not always trivial. Use of a second spacer is helpful under the above mentioned conditions as it can pillar the framework and imparts higher dimensionality. A multifunctional ligand with more than one functional group, such as carboxylate ($-CO_2$) and phosphonate ($-PO_3$), where the latter has the capability of binding more than one metal center, would be another choice to obtain higher dimensional frameworks. Here we have employed a bifunctional ligand, H_2-CEP, and allowed it to react with V^{IV} under hydrothermal conditions resulting in a 3D VO^{2+} framework **1**. Piperazine countercation acts as a structure-directing agent and balances the residual charge in the framework; the cation was generated under acidic conditions. X-ray single-crystal structural characterization reveals that compound **1** crystallizes in a monoclinic space group, $P2_1/n$. The asymmetric unit comprises one oxovanadium (VO^{2+}), one CEP ligand, half of a piperazine countercation, and one guest water molecule. Each V1 atom is octahedrally coordinated to one oxo group (O6), one chelated carboxylate group (O1 and O2), and three phosphonyl oxygens, O3, O4, and O5, from three different CEP ligands (Figure 1a). The V1−O bond lengths lies in the range of 1.958(4)−2.317(5) Å except V═O, which is 1.612(5) Å. Each V1 center in the structure locates itself in a highly distorted octahedral geometry, and the distortion is reflected in *cisoid* (60.58(15)°−109.2(2)°) and *transoid* angles (148.03(19)°−163.98(19)°). The PO_3^{2-} group of each CEP ligand binds three V1 centers in a tridentate fashion, while each carboxy group binds one V1 center in a bidentate fashion. The tridentate binding mode of PO_3^{2-} with V1 results an eight-membered ring containing two V centers, four oxygens, and two P atoms from two PO_3^{2-} groups (Figure 2a). The third oxygen atom of PO_3^{2-} group renders the eight-membered ring to progress in the crystallographic *a* direction to form a ladder-like structure where V1−O4−P1 acts as a rung of the ladder (Figure 2b). The ladders are connected to each other by CEP ligand with the aid of carboxylate coordination to V center to generate a 3D open framework structure (Figures 2c and 1b,c). Topological analysis with TOPOS 4.0[16] reveals that **1** is a four-connected net with Schläfli symbol $\{4^2\cdot 6^3\cdot 8\}$ (Figure 1d). The framework houses bidirectional channels: one hexagonal along the *a* direction occupied by H_2-PIP cations and the other along the [101] direction occupied by guest water molecules (Figure 1c and Figure S3, Supporting Information).

dx.doi.org/10.1021/ic200463k |*Inorg. Chem.* 2011, 50, 5145–5152

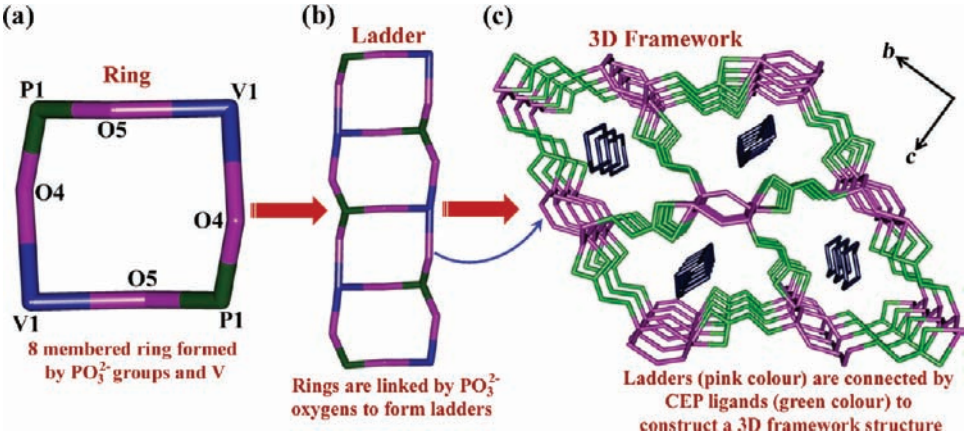

Figure 2. A simplified and stepwise demonstration of the construction of 3D framework of **1** from eight-membered rings and ladders. From the symmetry point of view, the ladders are generated in the unit cell by the successive application of 2_1 screw axis along *b* and by *n*-glide.

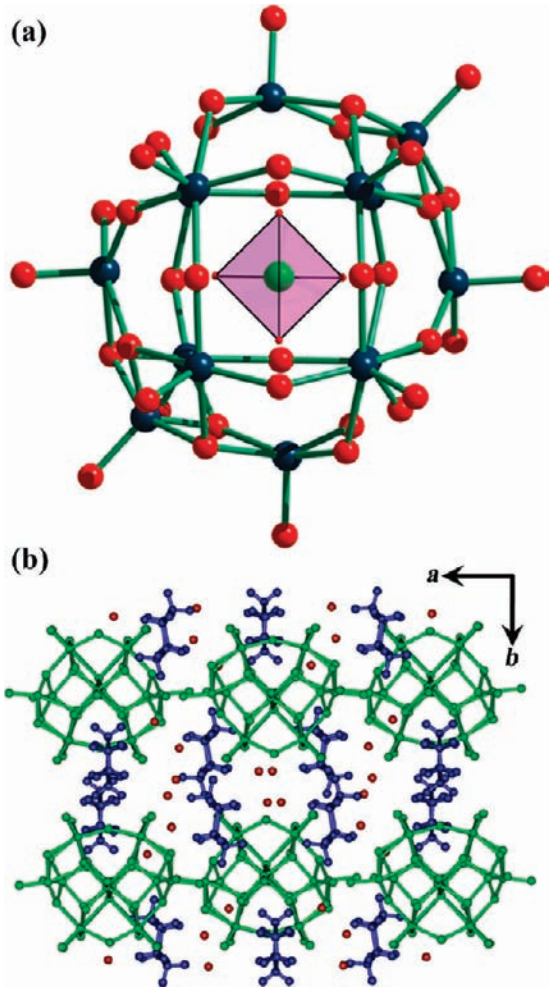

Figure 3. Crystal structure of the polyoxovanadate (**2**). (a) PO_4^{3-} anion sitting in the cavity of POV is shown in polyhedron view. Color specifications: vanadium, sky blue; oxygen, red; phosphorus, green. (b) Crystal packing of the cluster viewed along crystallographic *c* direction. Color specifications: POVs, green; H_2PIP cations, blue; guest water molecules, maroon.

A simplified demonstration of formation of the 3D framework of **1** is shown in Figure 2. The guest-free framework contains 33.9% void volume per unit cell volume (321 Å^3) as calculated by PLATON.[17]

Synthesis and Characterization of the Polyoxovanadate (POV), $[H_5(H_2PIP)_3]$ $[V^V_{12}V^{IV}_2O_{38}(PO_4)]\cdot 8H_2O$ (2). POVs are widely known to assemble in aqueous solution where pH of the reaction media (usually low pH) is always crucial.[18] Organic molecules as templates play a significant role in the formation of unusual structures of POVs;[19] a large number of clusters have been assembled with varying V^{4+}/V^{5+} through the linking of VO_x^{n+} polyhedra (tetrahedra, square-pyramids, and octahedra), using a variety of organic bases. In the case of POVs, in most cases, the structure-directing organic molecules are either found inside the cavity of the cluster or outside as countercations. N-containing ligands, such as ethylenediamine (en), tetramethylammonium (TMA), 1,4-diazabicyclooctane (DABCO), 2, 2′-bipyridine, etc., have been commonly employed as templates.[20] The geometry of the guest has been identified as the major influence in the formation of these POVs although in many instances the organic molecules merely appear as countercations. Although, several routes have been employed to obtain POVs with variety of structures, a MOF has never been used as a precursor to synthesize such cluster compounds. We have adopted a simple "top-down" approach for obtaining a POV by the reaction of the parent VMOF (**1**) with either $NaNO_3$ or $LiNO_3$ under aqueous solution at pH $\approx$ 2.1. At low pH, the VMOF disintegrates, and most probably, concomitant hydrolysis of the CEP ligand results in PO_4^{3-} anions (found to occupy the cavity of the cluster) that initiate the nucleation. Moreover, the VMOF also houses piperazine cations in the framework, a structure-directing agent for POVs. We believe it is the culmination of these two factors, formation of the PO_4^{3-} anion and presence of the piperazine cation in the framework, that provide the necessary driving force for the assembly of the present POV at the mentioned pH.

Single-crystal structural determination reveals that the compound **2** crystallizes in a monoclinic system with *C*2/*c* space group and consists of one $[V^V_{12}V^{IV}_2O_{38}(PO_4)]^{11-}$ moiety, three $(H_2PIP)^{6+}$ cations, five protons, and eight lattice water molecules. As shown in Figure 3a, the polyoxoanion $[V^V_{12}V^{IV}_2O_{38}(PO_4)]^{11-}$ is based on the well-known Keggin structure with seven pairs of four-coordinated terminal $\{VO^{2+}\}$ units where each V is five-coordinated and has a distorted square-pyramidal geometry. V−O bond distances and O−V−O bond angles are in the range

dx.doi.org/10.1021/ic200463k |*Inorg. Chem.* 2011, 50, 5145–5152

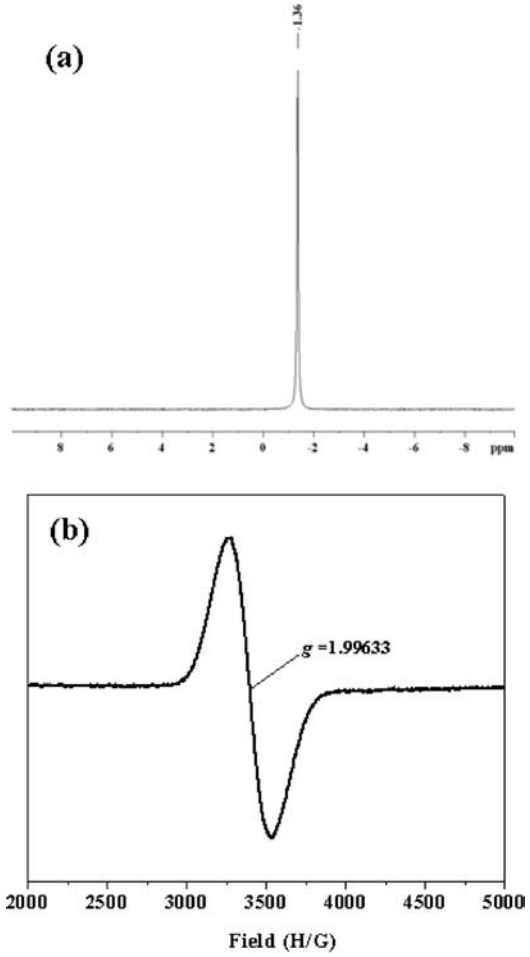

Figure 4. (a) ^{31}P NMR spectrum of compound **2**; (b) X-band EPR spectrum of solid sample of compound **2** at 295 K.

of 1.579(7)−2.384(6) Å and 72.3(2)°−169.4(3)°, respectively. The peripheral $\{VO_5\}$ square pyramids are connected with each other via two types of oxo-bridges (μ_2-O and μ_3-O bridge). The cluster houses a $\{PO_4\}^{3-}$ anion in its cavity (Figure 3a), which has several semibonding interactions (average V···O distance, 2.374 Å) with vanadium atoms of the POV. The presence of P in the cluster has been confirmed by ^{31}P NMR spectrum (Figure 4a) and EDX analysis (Figure S4, Supporting Information). The P−O distances are in the range of 1.526(6)−1.531(6) Å and the O−P−O angles vary from 109.1(3)° to 110.0(3)°. H_2PIP cations are intercalated between the polyoxoanions (Figure 3b) and are involved in several hydrogen bonding interactions resulting a 3D supramolecular structure (Figure S5, Supporting Information).

The assignments of oxidation states for the vanadium atoms are consistent with the overall charge balance of the compound and are confirmed by EPR (Figure 4b), magnetism (Figures S6 and S7, Supporting Information), and valence sum calculations. The EPR spectrum of compound **2** shows a sharp isotropic signal with a relatively small g value (g = 1.99633 at room temperature) indicating the existence of unpaired electrons.[21] Variable-temperature magnetic susceptibility of **2** was measured between 5 and 300 K, and the magnetic behavior in the form of χ_M vs T and $\chi_M T$ vs T are shown in Figure S6, Supporting Information. As can be seen from $\chi_M T$ vs T plot, the value of $\chi_M T$ (at 300 K 0.57 cm^3 mol^{-1} K) continuously decreases with temperature, and at 5 K, it

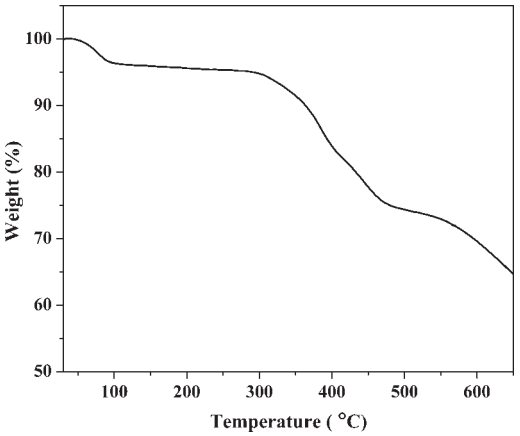

Figure 5. TGA of compound **1** carried out under N_2 atmosphere.

become 0.26 cm^3 mol^{-1} K. The $\chi_M{}^{-1}$ vs T plot is almost linear down to 30 K (Figure S7, Supporting Information) and follows the Curie−Weiss law with C = 0.5040 cm^3 mol^{-1} K and Weiss temperature θ = −1.19 K. These features indicate weak antiferromagnetic interaction operating in the cluster. The magnetic moment (μ_{eff}) calculated from susceptibility data turns out to be 2.15 μB at room temperature slightly lower than the theoretically calculated value of 2.84 μB for two unpaired spins. The observed magnetic moment, μ_{eff} suggests the presence of two V^{4+} centers in **2**. The lower value of μ_{eff} can be attributed to the delocalization of two unpaired electrons within the whole POV cluster. The valence sum calculations give values of 4.94, 5.26, 4.51, 4.92, 4.83, 4.95, and 4.88 for V(1), V(2), V(3), V(4), V(5), V(6), and V(7), respectively, with average value of 4.90 (the expected average value for $V^{5+}{}_{12}V^{4+}{}_2$ is 4.86). The valence sum calculation and μ_{eff} calculated from magnetic susceptibility data suggest that only 2 out of 14 vanadium atoms are in +4 oxidation states with two electrons delocalized within the whole POV cluster, which is also in concord with slightly lower g value calculated from EPR data.

Thermal and PXRD Analysis. To evaluate the thermal stability of the as-synthesised compound **1**, thermogravimetric analysis (TGA) was carried out in the temperature range 30−650 °C (Figure 5). Initial weight loss of ∼4.5 wt % in the temperature range 30−150 °C corresponds to the presence one guest water molecule in the structure. The profile then shows a long plateau, and the dehydrated compound, **1**′, $\{(H_2PIP)_{0.5}[VO(CEP)]\}$, is stable up to 290 °C and then starts decomposing to an unidentified phase.

The PXRD pattern of compound **1** in different states is shown in Figure 6. The very good correspondence between the simulated and as-synthesized patterns suggest the high purity of the bulk sample. PXRD pattern of the heated sample at 100 °C shows small shift in peak positions suggesting structural rearrangement upon loss of the lattice water molecule. The structural transformation is further confirmed by indexing the powder pattern of **1**′ by Dicvol91[22] program, which suggests a new monoclinic cell with parameters a = 17.214(17) Å, b = 11.879(8) Å, c = 15.553(13) Å, and β = 91.175(93)° (see Supporting Information). When the dehydrated sample is exposed to water vapor for 48 h, the original framework regenerates and is also confirmed by indexing (cell parameters: a = 6.373(8) Å; b = 8.982(9) Å; c = 16.753(19) Å; β = 100.788(183)°). Thus compound **1** is reversible with respect to dehydration−rehydration process.

dx.doi.org/10.1021/ic200463k |*Inorg. Chem.* 2011, 50, 5145–5152

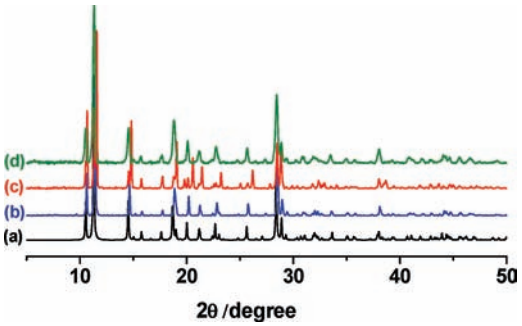

Figure 6. PXRD pattern of compound **1**: (a) simulated; (b) as-synthesized; (c) dehydrated at 100 °C; (d) rehydrated for 2 days. Similarity in simulated and as-synthesized pattern indicates high purity of the compound.

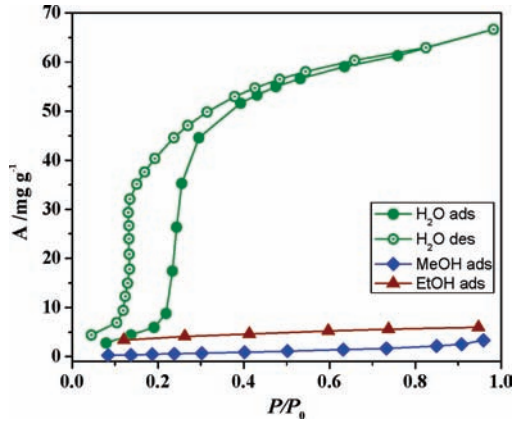

Figure 7. Solvent adsorption profiles of **1**: H_2O and EtOH at 298 K and MeOH at 293 K. P_0 is the saturated vapor pressure of the adsorbates at the measurement temperature. Closed symbols indicate adsorption and open symbols desorption.

Adsorption Study. Gas adsorption studies, such as N_2 (kinetic diameter, 3.64 Å) at 77 K and CO_2 (kinetic diameter, 3.3 Å) at 195 K, with **1′** reveal no uptake suggesting a nonporous phase of the framework (Figure S8, Supporting Information). Adsorption studies with different solvent vapors were carried out with **1′** to get an understanding about the affinity of the framework toward small molecules. No guest inclusion was observed at very low pressure and ambient temperature, which suggest a nonporous phase of the framework. However, very interestingly as the pressure increases and reaches $P/P_0 \approx 0.2$, a gate-opening behavior was noticed in H_2O (kinetic diameter, 2.68 Å) adsorption isotherm (Figure 7). With MeOH (kinetic diameter, 4.0 Å) and EtOH (kinetic diameter, 4.3 Å) even at higher pressures, no uptake was recorded. This suggests hydrophilic nature of the compound because it adsorbs molecules of H_2O selectively over MeOH and EtOH vapors. The noninclusion of N_2, CO_2, and solvent molecules, MeOH and EtOH, can be correlated to larger size of the adsorbates compared with the channel size and dynamic nature of the framework. The gate-opening behavior of H_2O adsorption profile (Figure 7) can be explained as follows. The PXRD pattern of **1′** exhibits small changes in the peak positions as well as appearance of some new peaks suggesting structural rearrangement upon dehydration. This suggests the dynamic nature of the framework **1** and is perceivable because of the presence of a flexible ethyl group in the CEP ligand that can

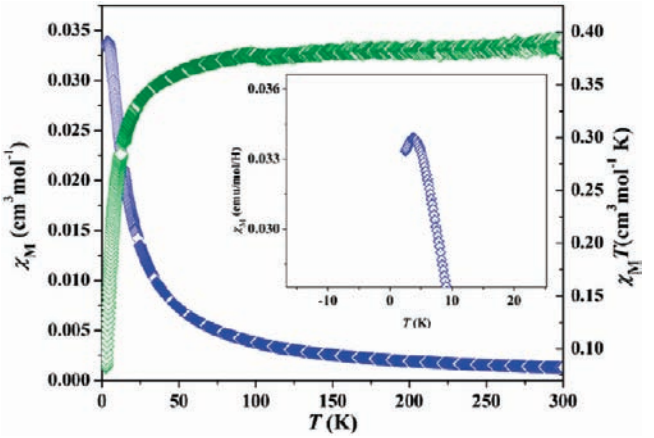

Figure 8. Plot of molar magnetic susceptibility, χ_M, and $\chi_M T$ as a function of T for **1** at 1 KOe. Inset: enlarged view of χ_M vs T plot showing antiferromagnetic ordering at 3.8 K.

relax upon guest evacuation and subsequently block the pore. Hence, initially at very low P/P_0, it is difficult for the H_2O molecules to penetrate into the framework. However, as the pressure increases to $P/P_0 \approx 0.2$, the H_2O molecules start to penetrate into the framework because of the enhanced adsorbate−adsorbent interaction, and the adsorption curve shows a steep rise. The H_2O adsorption profile becomes almost saturated at higher P/P_0 and ends with a maximum uptake of 83 mL/g. The maximum uptake corresponds to 1 mol of H_2O per formula unit of **1′**. The desorption profile does not trace the adsorption profile and shows small hysteresis, which also suggests structural transformation upon dehydration−rehydration.

Magnetic Properties of 1. The temperature dependence of the magnetic susceptibilities for **1** in the temperature range 2.5−300 K under a 1 kOe applied field was measured using a Quantum Design PPMS magnetometer. The $\chi_M T$ value at 300 K is about 0.39 $cm^3\ mol^{-1}\ K$ ($\chi_M = 0.0013\ cm^3\ mol^{-1}$), close to the spin only value (0.37 $cm^3\ mol^{-1}\ K$) expected for a magnetically isolated V^{4+} with $g = 2.0$. As the temperature is lowered, $\chi_M T$ is almost constant to 60 K (0.37 $cm^3\ mol^{-1}\ K$) and then decrease rapidly to 0.08 $cm^3\ mol^{-1}\ K$ at 2.5 K (Figure 8). Moreover χ_M increases gradually with decreasing temperature and reaches maximum of 0.0034 $cm^3\ mol^{-1}\ K$ at 3.4 K, and then χ_M value decreases to 0.033 at 2.5 K. The $\chi_M{}^{-1}$ vs T plot is almost linear down to 30 K (Figure S9, Supporting Information) and follows the Curie−Weiss law with $C = 0.39\ cm^3\ mol^{-1}\ K$ and Weiss temperature $\theta = -4.32$ K. This feature clearly indicates that antiferromagnetic interaction is operating between the V^{4+} centers bridged by the $PO_3{}^{2-}$ units. The $M-H$ curve at 2.5 K is almost linear reaching a maximum value of 0.26 Nβ at 50 kOe, which is markedly below the expected value for a V^{4+} with $S = {}^1/_2$ (Figure S10, Supporting Information). Taking into account the structural features of compound **1**, further inspection of the magnetic behaviors is worthwhile. The $PO_3{}^{2-}$ unit of the linker CEP connects three V^{4+} centers forming a 1D ladder-like structure; four ladders are connected to each other through the linker forming a 3D framework (Figure 1c). In the 1D ladder, P centers and V^{4+} centers are alternately positioned and VOP forms the rungs of the ladder. Further inspection suggests that such arrangements of the V centers in the ladders form alternative triangles of V^{4+} (Figure 9), which are inherently frustrated, which is clear in the corresponding feature of $\chi_M T$ vs

dx.doi.org/10.1021/ic200463k |*Inorg. Chem.* 2011, 50, 5145–5152

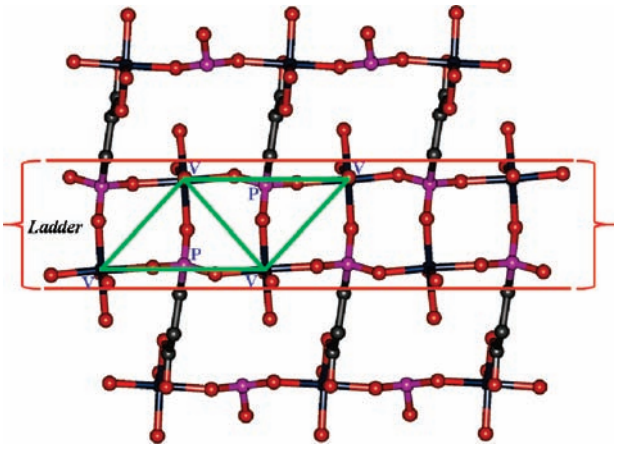

Figure 9. Figure showing the ladder-like structure formed by PO_3^{2-} group of CEP ligand and V^{4+} center. The V^{4+} ions lie on the vertices of the triangle.

T and *M* vs *H* curves.[23] It has been stated that magnetic frustration can suppress or significantly reduce long-range ordering. Experimentally, the degree of frustration in an antiferromagnet is defined by the ratio of the Weiss constant to the ordering temperature, $f = [\theta]/T_N$.[23b,c] For compound **1**, it is 1.4, which suggests that frustration is very small in this system. The observed low-temperature drop in χ_M for **1** suggests that the net spin moment is suppressed by interladder antiferromagnetic interactions through the CEP ligand leading to the 3D antiferromagnetic ordering at $T = 3.8$ K.

CONCLUSION

In summary, we have synthesized a 3D metal−organic framework of vanadium using a doubly functionalized linker, H_2-CEP (carboxy and phosphonyl), under hydrothermal conditions. The framework shows high thermal stability and a highly selective gated water adsorption property among a number of gases (N_2, CO_2) and solvent molecules (MeOH, EtOH). The adsorption behavior is correlated by smaller channel aperture and dynamic nature of the framework. The framework exhibits antiferromagnetic ordering at low temperature through superexchange processes between the V^{4+} centers bridged by PO_3^{2-} moieties. For the first time, we have shown that a simple 3D VMOF can act as an eloquent precursor for a novel POV cluster. Our simple approach would open up new directions toward synthetic methodologies of novel polyoxometalate clusters.

EXPERIMENTAL SECTION

Materials. All the chemicals and reagents were commercially available and used as supplied without further purification. $VOSO_4 \cdot xH_2O$, 2-carboxyethylphosphonic acid, piperazine, and hydrofluoric acid (35%) were obtained from Aldrich Chemical Co..

Physical Measurements. The elemental analysis was carried out using a Thermo Fischer Flash 2000 Elemental Analyzer. IR spectra were recorded on a Bruker IFS 66v/S spectrophotometer using KBr pellets in the region 4000−400 cm^{-1}. Thermogravimetric analysis (TGA) was carried out on a METTLER TOLEDO TGA850 instrument in the temperature range 30−650 °C under nitrogen atmosphere (flow rate of 50 mL/min) at a heating rate of 5 °C/min. Powder X-ray diffraction (PXRD) patterns were recorded on a Bruker D8 Discover instrument using Cu Kα radiation. EPR measurements were carried out in a Bruker spectrometer in *X* band with microwave frequency of 9.43 GHz at RT. ^{31}P NMR spectrum was recorded on a Bruker AV-400 spectrometer with 85% H_3PO_4 as internal standard.

Magnetic Measurements. DC magnetic susceptibility data of powdered crystalline samples of **1** and **2** were collected on a vibrating sample magnetometer, PPMS (Physical Property Measurement System, Quantum Design, USA), in the temperature range 2.5−300 K (5−300 K for **2**) with applied field of 1000 Oe (500 Oe for **2**). Field variation (−5 to 5 kOe) magnetization measurement was carried out at 2.5 K.

Adsorption Measurements. CO_2 at 195 K and N_2 at 77 K adsorption studies with the dehydrated sample of **1** prepared at 373 K under high vacuum were carried out using QUANTACHROME QUADRASORB-*SI* analyzer. Dead volume of the sample cell was measured using helium gas of 99.999% purity. The adsorption isotherm of different solvents (like H_2O and EtOH at 298 K and MeOH at 293 K) were measured in the vapor state by using BELSORP-aqua volumetric adsorption instrument from BEL, Japan. In the sample chamber (∼12 mL) maintained at $T \pm 0.03$ K was placed the adsorbent sample (100−150 mg), which had been prepared at 373 K at 10^{-1} Pa for about 12 h prior to measurement of the isotherms. The adsorbate was charged into the sample tube, and then the change of the pressure was monitored, and the degree of adsorption was determined by the decrease in pressure at the equilibrium state. All operations were computer-controlled and automatic.

Synthesis of $\{(H_2PIP)_{0.5}[VO(CEP)] \cdot H_2O\}$ (1). $VOSO_4$ (0.196 g, 1.2 mmol), 2-carboxyethylphosphonic acid (H_2-CEP) (0.166 g, 1.08 mmol), and piperazine (PIP) (0.103 g, 1.2 mmol) were taken in a 23 mL Teflon bomb, and to it 14 mL of H_2O was added and the mixture was stirred for half an hour. To this solution, then two drops of hydrofluoric acid (35%) was added to adjust the pH to ∼5. Then the Teflon bomb was placed in a stainless steel reactor and heated at 180 °C for 170 h. After completion of the reaction, the reactor was cooled to RT for 12 h. Good quality light green crystals together with some green precipitates were obtained. The crystals were separated, and a suitable crystal was mounted for single-crystal data. Yield: 35%, relative to V. Anal. Calcd for $C_5H_{12}VNO_7P$: C, 21.44; H, 4.32; N, 5.00. Found: C, 21.14; H, 3.97; N, 4.55. FT−IR (KBr pellet, 4000−400 cm^{-1}): ν(V═O), 952; ν(V−O−V), 815, 749, 717, 614; ν(C═O), 1528, 1454; $\nu(CPO_3)$, 1056, 1018; ν(lattice H_2O), 3624 (Figure S1, Supporting Information). The vibrations at 3059, 2937, 2829, 1578, 1542, 1412, 1325, 1217, and 1123 cm^{-1} in the IR spectrum of **1** can be regarded as features of the piperazine cations. The purity of the product was confirmed from similarity of PXRD patterns of the bulk phase with the simulated pattern.

Synthesis of $[H_5(H_2PIP)_3][V^V_{12}V^{IV}_2O_{38}(PO_4)] \cdot 8H_2O$ (2). Compound **2** was synthesized by the following procedure. $\{(H_2PIP)_{0.5}[VO(CEP)] \cdot H_2O\}$ (**1**; 0.027 g) was added to a 20 mL of 1 M $NaNO_3/LiNO_3$ solution at room temperature, and the resulting solution was stirred for 24 h at pH ≈ 2.1. Then the reaction mixture was filtered and left open in air for crystallization. After ∼10 days black colored crystals were obtained at pH ≈ 2.1. Yield: 17%, relative to V. Anal. Calcd for $C_{12}H_{57}V_{14}N_6O_{50}P$: C, 7.88; H, 3.14; N, 4.59; Found: C, 7.95; H, 3.01; N, 4.27. FT-IR (KBr pellet, 4000−400 cm^{-1}): ν(P−O), 1055; ν(V═O_t), 942; ν(V−O_b−V), 763, 710; ν(V−O_c−V), 586, 534; ν(lattice H_2O), 3516; The vibrations at 3314, 3255, 3003, 2906, 1581, 1456, and 1384 cm^{-1} in the IR spectrum of **2** can be regarded as features of the piperazine cations (Figure S2, Supporting Information).

Single-Crystal X-ray Diffraction. Suitable single crystals of **1** and **2** were mounted on a thin glass fiber with commercially available super glue. X-ray single crystal structural data was collected on a Bruker Smart−CCD diffractometer equipped with a normal focus, 2.4 kW sealed tube X-ray source with graphite monochromated Mo Kα radiation (λ = 0.71073 Å) operating at 50 kV and 30 mA. Crystal data was collected at 298 K. The program SAINT[24] was used for integration of diffraction profiles and absorption correction was made with SADABS

Table 1. Crystal Data and Structure Refinement Parameters for 1 and 2

parameters	1	2
empirical formula	$C_5H_{12}VNO_7P$	$C_{12}H_{57}V_{14}N_6O_{50}P$
formula weight	280.05	1829.75
cryst. syst.	monoclinic	monoclinic
space group	$P2_1/n$	$C2/c$
a, Å	6.3846(5)	19.206(4)
b, Å	16.7722(19)	20.886(4)
c, Å	8.9996(12)	13.397(3)
α, deg	90	90
β, deg	100.121(8)	110.247(7)
γ, deg	90	90
V, Å^3	948.72(18)	5042.0(18)
Z	4	4
T, K	298	298
μ, mm^{-1}	1.231	2.626
D_{calcd}, g/cm^3	1.947	2.367
F (000)	564	3500
reflns $[I > 2\sigma(I)]$	1352	1931
unique reflns	2448	2681
measured reflns	12711	20434
R_{int}	0.148	0.108
GOF on F^2	1.07	1.13
$R_1[I > 2\sigma(I)]^a$	0.0751	0.0574
$R_w[I > 2\sigma(I)]^b$	0.2081	0.1823
$\Delta\rho$ max, min [e Å^{-3}]	1.13, −0.80	1.40, −1.46

$^a R = \Sigma||F_o| - |F_c||/\Sigma|F_o|$. $^b R_w = [\Sigma\{w(F_o^2 - F_c^2)^2\}/\Sigma\{w(F_o^2)^2\}]^{1/2}$.

program.[25] The structures were solved by SIR 92[26] and refined by full-matrix least-squares method using SHELXL 97.[27] The non-hydrogen atoms were refined anisotropically. The hydrogen atoms were fixed by HFIX and placed in the ideal positions. Potential solvent-accessible area or void space was calculated using the PLATON[17] multipurpose crystallographic software. All crystallographic and structure refinement data of the compounds are summarized in Table 1. Selected bond distances and angles are given in Table S2, Supporting Information. All calculations were carried out using SHELXL 97,[27] PLATON,[17] SHELXS 97,[28] and WinGX system, ver 1.70.01.[29]

■ ASSOCIATED CONTENT

Supporting Information. X-ray crystallographic files in CIF format for the two compounds, IR spectra, molecular figures, magnetic plots, and bond length/bond angle tables for compounds **1** and **2** and gas adsorption profiles of **1**. This material is available free of charge via the Internet at http://pubs.acs.org.

■ AUTHOR INFORMATION

Corresponding Author

*E-mail: tmaji@jncasr.ac.in. Phone: +91 80 2208 2826. Fax: +91 80 2208 2766.

Author Contributions

‡Authors contributed equally.

■ ACKNOWLEDGMENT

The authors are thankful to Prof. S. V. Bhat of Indian Institute of Science, Bangalore, for helping with EPR measurements. We also thank Prof. A Sundaresan and Mr. Nitesh Kumar of JNCASR, Bangalore, for magnetic measurements. P.K. acknowledges CSIR, India for a senior research fellowship. A.C.G. is thankful to JNCASR for SRFP program.

■ REFERENCES

(1) (a) Kitagawa, S.; Kitaura, R.; Noro, S. *Angew. Chem., Int. Ed.* **2004**, *43*, 2334. (b) Rao, C. N. R.; Natarajan, S.; Vaidhyanathan, R. *Angew. Chem., Int. Ed.* **2004**, *43*, 1466. (c) Kitagawa, S.; Matsuda, R. *Coord. Chem. Rev.* **2007**, *251*, 2490. (d) Maji, T. K.; Kitagawa, S. *Pure Appl. Chem.* **2007**, *79*, 2155. (e) Férey, G. *Chem. Soc. Rev.* **2008**, *37*, 191. (f) Shimizu, G. K. H.; Vaidhyanathan, R.; Taylor, J. M. *Chem. Soc. Rev.* **2009**, *38*, 1430. (g) Natarajan, S.; Mahata, P. *Chem. Soc. Rev.* **2009**, *38*, 2304. (h) Chen, B. L.; Xiang, S. C.; Qian, G. D. *Acc. Chem. Res.* **2010**, *43*, 1115. (i) Meek, S. T.; Greathouse, J. A.; Allendorf, M. D. *Adv. Mater.* **2011**, *23*, 249.

(2) (a) Dybtsev, D. N.; Chun, H.; Yoon, S. H.; Kim, D.; Kim, K. *J. Am. Chem. Soc.* **2004**, *126*, 32. (b) Pan, L.; Parker, B.; Huang, X.; Olson, D. H.; Lee, J. Y.; Li, J. *J. Am. Chem. Soc.* **2006**, *128*, 4180. (c) Dincã, M.; Yu, A. F.; Long, J. R. *J. Am. Chem. Soc.* **2006**, *128*, 8904. (d) Ma, S.; Sun, D.; Simmons, J. M.; Collier, C. D.; Yuan, D.; Zhou, H. -C. *J. Am. Chem. Soc.* **2008**, *130*, 1012. (e) Kanoo, P.; Matsuda, R.; Higuchi, M.; Kitagawa, S.; Maji, T. K. *Chem. Mater.* **2009**, *21*, 5860. (f) Kanoo, P.; Gurunatha, K. L.; Maji, T. K. *J. Mater. Chem.* **2010**, *20*, 1322.

(3) (a) Hasegawa, S.; Horike, S.; Matsuda, R.; Furukawa, S.; Mochizuki, K.; Kinoshita, Y.; Kitagawa, S. *J. Am. Chem. Soc.* **2007**, *129*, 2607. (b) Alaerts, L.; Maes, M.; Giebeler, L.; Jacobs, P. A.; Martens, J. A.; Denayer, J. F. M.; Kirschhock, C. E. A.; De Vos, D. E. *J. Am. Chem. Soc.* **2008**, *130*, 14170. (c) Choi, H. S.; Suh, M. P. *Angew. Chem., Int. Ed.* **2009**, *48*, 6865. (d) Cheon, Y. E.; Park, J.; Suh, M. P. *Chem. Commun.* **2009**, 5436.

(4) (a) Abrahams, B. F.; Moylan, M.; Orchard, S. D.; Robson, R. *Angew. Chem., Int. Ed.* **2003**, *42*, 1848. (b) Horike, S.; Tanaka, D.; Nakagawa, K.; Kitagawa, S. *Chem. Commun.* **2007**, 3395. (c) Maji, T. K.; Matsuda, R.; Kitagawa, S. *Nat. Mater.* **2007**, *6*, 142. (d) Gurunatha, K. L.; Uemura, K.; Maji, T. K. *Inorg. Chem.* **2008**, *47*, 5678. (e) Zhang, J.-P.; Chen, X.-M. *J. Am. Chem. Soc.* **2008**, *130*, 6010.

(5) (a) Seo, J. S.; Whang, D.; Lee, H.; Jun, S. I.; Oh, J.; Jeon, Y. J.; Kim, K. *Nature* **2000**, *404*, 982. (b) Wu, C. D.; Hu, A.; Zhang, L.; Lin, W. B. *J. Am. Chem. Soc.* **2005**, *127*, 8940. (c) Dybtsev, D. N.; Nuzhdin, A. L.; Chun, H.; Bryliakov, K. P.; Talsi, E. P.; Fedin, V. P.; Kim, K. *Angew. Chem., Int. Ed.* **2006**, *45*, 916. (d) Horike, S.; Dincã, M.; Tamaki, K.; Long, J. R. *J. Am. Chem. Soc.* **2008**, *130*, 5854.

(6) (a) Pârvulescu, A. N.; Marin, G.; Suwinska, K.; Kravtsov, V. C.; Andruh, M.; Pârvulescu, V.; Pârvulescu, V. I. *J. Mater. Chem.* **2005**, *15*, 4234. (b) Tzeng, B.-C.; Chiu, T.-H.; Chen, B.-S.; Lee, G.-H. *Chem.—Eur. J.* **2008**, *14*, 5237. (c) Plabst, M.; McCusker, L. B.; Bein, T. *J. Am. Chem. Soc.* **2009**, *131*, 18112.

(7) (a) Qiu, L. G.; Li, Z. Q.; Wu, Y.; Wang, W.; Xu, T.; Jiang, X. *Chem. Commun.* **2008**, 3642. (b) Chen, B. L.; Wang, L. B.; Zapata, F.; Qian, G. D.; Lobkovsky, E. B. *J. Am. Chem. Soc.* **2008**, *130*, 6718. (c) Chen, B. L.; Wang, L. B.; Xiao, Y. Q.; Fronczek, F. R.; Xue, M.; Cui, Y. J.; Qian, G. D. *Angew. Chem., Int. Ed.* **2009**, *48*, 500. (d) Xie, Z. G.; Ma, L. Q.; dekrafft, K. E.; Jin, A.; Lin, W. B. *J. Am. Chem. Soc.* **2010**, *132*, 922.

(8) (a) Horcajada, P.; Serre, C.; Maurin, G.; Ramsahye, N. A.; Balas, F.; Vallet-Regi, M.; Sebban, M.; Taulelle, F.; Férey, G. *J. Am. Chem. Soc.* **2008**, *130*, 6774. (b) Horcajada, P.; Serre, C.; Vallet−Regí, M.; Sebban, M.; Taulelle, F.; Férey, G. *Angew. Chem., Int. Ed.* **2006**, *45*, 5974.

(9) (a) Riou-Cavellec, M.; Sanselme, M.; Férey, G. *J. Mater. Chem.* **2000**, *10*, 745. (b) Zhang, X.-M.; Hou, J.-J.; Zhang, W.-X.; Chen, X.-M. *Inorg. Chem.* **2006**, *45*, 8120. (c) Ouellette, W.; Yu, M. H.; O'Connor, C. J.; Zubieta, J. *Inorg. Chem.* **2006**, *45*, 7628. (d) Rocha, J.; Almeida Paz,

F. A.; Shi, F.-N.; Ferreira, R. A. S.; Trindade, T.; Carlos, L. D. *Eur. J. Inorg. Chem.* **2009**, 4931.

(10) Barthelet, K.; Marrot, J.; Riou, D.; Férey, G. *Angew. Chem., Int. Ed.* **2002**, *41*, 281.

(11) (a) Alaerts, L.; Kirschhock, C.; Maes, M.; van der Veen, M.; Finsy, V.; Depla, A.; Martens, J.; Baron, G.; Jacobs, P.; Denayer, J.; De Vos, D. *Angew. Chem., Int. Ed.* **2007**, *46*, 4293. (b) Meilikhov, M.; Yusenko, K.; Fischer, R. A *Dalton Trans.* **2010**, *39*, 10990.

(12) (a) Chen, C.-L.; Goforth, A. M.; Smith, M. D.; Su, C.-Y.; zur Loye, H.-C. *Angew. Chem., Int. Ed.* **2005**, *44*, 6673. (b) Dai, L.-M.; You, W.-S.; Li, Y.-G.; Wang, E.-B.; Huang, C.-Y. *Chem. Commun.* **2009**, 2721. (c) Thomas, J.; Agarwal, M.; Ramanan, A.; Chernov, N.; Whittingham, M. S. *CrystEngComm* **2009**, *11*, 625. (d) de Luis, R. F; Urtiaga, M. K.; Mesa, J. L.; Aguayo, A. T.; Rojo, T.; Arriortua, M. I. *CrystEngComm* **2010**, *12*, 1880. (e) Liu, Y.-B.; Cui, X.-B.; Xu, J.-Q.; Lu, Y.-K.; Liu, J.; Zhang, Q.-B.; Wang, T.-G. *J. Mol. Struct.* **2006**, *825*, 45. (f) Li, F.; Xu, L.; Wei, Y.; Wang, E. *Inorg. Chem. Commun.* **2005**, *8*, 263.

(13) (a) Liu, C. M.; Zhang, J. Y.; Zhang, D. Q. *J. Coord. Chem.* **2008**, *61*, 627. (b) Zhang, C. D.; Liu, S. X.; Gao, B.; Sun, C. Y.; Xie, L. H.; Yu, M.; Peng, J. *Polyhedron* **2007**, *26*, 1514. (c) Arumuganathan, T.; Das, S. K. *Inorg. Chem.* **2009**, *48*, 496. (d) Shivaiah, V.; Reddy, P. V. N.; Cronin, L.; Das, S. K. *J. Chem. Soc., Dalton Trans.* **2002**, 3781.

(14) (a) Pradeep, C. P.; Long, D. L.; Streb, C.; Cronin, L. *J. Am. Chem. Soc.* **2008**, *130*, 14946. (b) Hasenknopf, B. *Front. Biosci.* **2005**, *10*, 275. (c) Vasylyev, M. V.; Neumann, R. *J. Am. Chem. Soc.* **2004**, *126*, 884. (d) Mbomekalle, I. M.; Keita, B.; Nadjo, L.; Berthet, P.; Hardcastle, K. I.; Hill, C. L.; Anderson, T. M. *Inorg. Chem.* **2003**, *42*, 1163. (e) Duraisamy, T.; Ojha, N.; Ramanan, A.; Vittal, J. J. *Chem. Mater.* **1999**, *11*, 2339. (f) Kiebach, R.; Näther, C.; Kögerler, P.; Bensch, W. *Dalton Trans.* **2007**, 3221.

(15) (a) Zheng, S.-T.; Yang, G.-Y. *Dalton Trans.* **2010**, *39*, 700. (b) Dolbecq, A.; Dumas, E.; Mayer, C. R.; Mialane, P. *Chem. Rev.* **2010**, *110*, 6009. (c) Hou, G. F.; Bi, L. H.; Li, B.; Wu, L. X. *Inorg. Chem.* **2010**, *49*, 6474.

(16) (a) Blatov, V. A.; Carlucci, L.; Ciani, G.; Proserpio, D. M. *CrystEngComm* **2004**, *6*, 377. (b) Blatov, V. A.; Shevchenko, A. P.; Serezhkin, V. N. *J. Appl. Crystallogr.* **2000**, *33*, 1193.

(17) Spek, A. L. *J. Appl. Crystallogr.* **2003**, *36*, 7.

(18) Pradeep, C. P.; Long, D.-L.; Streb, C.; Cronin, L. *J. Am. Chem. Soc.* **2008**, *130*, 14946.

(19) Muller, A.; Reuter, H.; Dillinger, S. *Angew. Chem., Int. Ed. Engl.* **1995**, *34*, 2328 and references therein..

(20) (a) Zhang, Y.; Zapf, P. J.; Meyer, L. M.; Haushalter, R. C.; Zubieta, J. *Inorg. Chem.* **1997**, *36*, 2159. (b) Zhang, Y.; Haushalter, R. C.; Clearfield, A. *Inorg. Chem.* **1996**, *35*, 4950. (c) Chirayil, T. G.; Boylan, T. A.; Mamak, M.; Zavalij, P. Y.; Whittingham, M. S. *J. Chem. Soc., Chem. Commun.* **1997**, 33. (d) Zhang, Y.; Haushalter, R. C.; Clearfield, A. *J. Chem. Soc., Chem. Commun.* **1996**, 1055.

(21) Patra, S. C.; Biswas, M. K.; Maity, A. N.; Ghosh, P. *Inorg. Chem.* **2011**, *50*, 1331.

(22) Louer, D.; Boultif, A. *J. Appl. Crystallogr.* **1991**, *24*, 987.

(23) (a) Kanoo, P.; Madhu, C.; Mostafa, G.; Maji, T. K.; Sundaresan, A.; Pati, S. K.; Rao, C. N. R. *Dalton Trans.* **2009**, 5062. (b) Ramirez, A. P. *Annu. Rev. Mater. Sci.* **1994**, *24*, 453. (c) Pati, S. K.; Rao, C. N. R. *Chem. Commun.* **2008**, 4683.

(24) SAINT+, 6.02 ed.; Bruker AXS: Madison, WI, 1999.

(25) Sheldrick, G. M. *SADABS, Empirical Absorption Correction Program*; University of Göttingen, Göttingen, Germany, 1997.

(26) Altomare, A.; Cascarano, G.; Giacovazzo, C.; Gualaradi, A. *J. Appl. Crystallogr.* **1993**, *26*, 343.

(27) Sheldrick, G. M. , University of Göttingen, Germany, 1997.

(28) Sheldrick, G. M. , University of Göttingen, Germany, 1997.

(29) Farrugia, L. J. *J. Appl. Crystallogr.* **1999**, *32*, 837.